ROSE 2008 – IEEE International Workshop
on Robotic and Sensors Environments
Ottawa – Canada, 17-18 October 2008

Evaluation of Growing Neural Gas Networks for Selective 3D Scanning

Ana-Maria Cretu, Emil M. Petriu, Pierre Payeur
School of Information Technology and Engineering
University of Ottawa
Ottawa, ON, CANADA, K1N 6N5
[acretu, petriu, ppayeur]@site.uottawa.ca

Abstract *– This paper addresses the issue of intelligent sensing for advanced robotic applications and is a continuation of our research in the area of innovative approaches for automatic selection of regions of observation for fixed and mobile sensors to collect only relevant measurements without human guidance. The growing neural gas network solution proposed here for adaptively selecting regions of interest for further sampling from a cloud of sparsely collected 3D measurements provides several advantages over the previously proposed neural gas solution in terms of user intervention, size of resulting scan and training time. Experimental results and comparative analysis are presented in the context of selective vision sampling.*

Keywords *– Selective sensing, 3D vision, neural gas network, growing neural gas network, feature detection, surface modeling.*

I. INTRODUCTION

Reducing the complexity of the large datasets provided by the current generation of 3D data acquisition devices (e.g. laser scanners) is one of the key techniques required in order to operate subsequent applications on the resulting data at a reasonable computational cost. The most widely exploited trend in contemporary literature involves the post-processing of data obtained by acquisition devices based on the user input of parameters such as the desired density of sampling, the regularity of sampling, or the minimum distance between samples. As the user is not always aware of the appropriate level of accuracy required for a model in order to be further processed, the adjustment of such parameters can be a difficult task associated with lengthy trial-and-error processes to fine tune the acquisition system.

This work is a continuation of our research on innovative approaches to achieve automatic selection of regions of observation for vision sensors to collect only relevant measurements without human guidance. The relevant regions of interest are extracted from 3D point clouds during the acquisition procedure to prevent a large amount of data from being collected and the associated excessive processing load. Starting from an initial, fast, and sparse scan of an object, a growing neural gas network map is used to adaptively select areas of interest for further scanning in order to improve the accuracy of the model. The final representation is a multi-resolution model with a higher resolution in areas rich in geometrical features.

The paper starts by presenting a brief literature review for the sampling and post-processing of large datasets in Section II. Our proposed solution for selective sensing based on a growing neural gas is shown in Section III. Experimental results for data sampling using vision sensors as well as a comparative analysis with our previous solution based on a neural gas network are presented in Section IV and V, respectively.

II. LITERATURE REVIEW

The most commonly encountered type of sampling procedure in the literature is stratified sampling, a technique that implies the collection of evenly spaced samples by subdividing the sampling domain into non-overlapping clusters and by sampling independently from each partition. Such a method ensures that an adequate sampling is applied to all partitions and is often exploited in the context of post-processing of large point clouds or meshes [1-7], where a subdivision of models into grid cells occurs and sample points that fall into the same cell are replaced by a common representative.

The 3D model is first voxelized with an octree and one sample is outputted for each voxel. The common representative for a voxel can be selected according to a probability that decays as the distance of the sample to the center of the voxel increases [1], and can be chosen to be the measured point that is closest to the average of points that fall into the same voxel [2] or the point whose normal is closest to the average of the points in the same voxel [3]. Alternatively principal component analysis can performed for each cell of the octree to efficiently decimate data [4].

Surface-based clustering can be employed as well instead of volumetric voxelization, where clusters are built by collecting neighboring samples while taking into account local sampling density [5]. Points are incrementally added to a cluster until a maximum size and/or a maximum allowed variation is reached.

Another category of solutions for the decimation of large datasets is based on boundary segmentation [6, 7]. Meshes are segmented into the boundary of the original domain and interior samples, and each part is simplified separately.

All the above methods are not meant to be incorporated in the actual sampling procedure, but rather to post-process collected data. An approach to integrate the sampling procedure into the measurement process is proposed by Pai *et al.* [8, 9] who consider a known mesh of the object under study, as well as a set of parameters such as the maximum force exerted on the object, the maximum probing depth and

978-1-4244-2595-2/08/$25.00 ©2008 IEEE

the number of steps for the deformation measurement. During probing, an algorithm generates the next position and orientation for the probe based on the specifications and the mesh of the object under test. It performs at the same time proximity checks and verifies the expected contact location of the probe with the mesh based on line intersection. However, the procedure is not selective and therefore is similar to collecting data for all the points of the mesh and can take very long. More recently, an adaptive scanning procedure was introduced by MacKinnon *et al.* [10] that builds upon a group of intermediate quality metrics to monitor several aspects of the scanning procedure, including outliers, aliasing, planarity, resolvability and reflectivity of the surface. This heuristic approach helps at focusing a laser scanner over an optimal field of view and guides the collection of 3D points over regions that will most likely maximize the visual quality of a final 3D model of an object while minimizing the number of measurements required. This approach is mainly evaluated in the context of high-resolution modeling of artefact objects, where the necessary information to compute the quality metrics is typically available and reliable.

III. PROPOSED FRAMEWORK

Our proposed framework is meant to be incorporated directly in the sampling procedure, with the purpose to achieve automated selective scanning over large workspaces. It uses a self-organizing neural network architecture that adaptively selects regions of interest for further refinement from a cloud of 3D sparsely collected measurements. Starting from an initial low resolution scan of an object, a growing neural gas network is employed to model the resulting point cloud and those regions that are worth further sampling in order to ensure an accurate model are detected by finding higher density areas in the resulting growing neural gas map. Rescanning at higher resolution is performed for each identified region and a multi-resolution model is then built using the initial sparse model and augmenting it by the high resolution regions of interest.

The approach is similar to the one previously proposed on the topic [11]. However, the work presented here tackles some of the limitations of the neural gas solution introduced in [11], particularly the one related to the need of the map size to be decided prior to learning. This size constrains the resulting mapping as well as the accuracy of the modeling results. Growing networks add incrementally nodes into the network structure, therefore eliminating the need for fixed size network maps.

A. Growing Neural Gas Networks

The use of self-organizing architectures in the context of selective 3D scanning is justified by their ability to quantize the given input space into clusters of points with similar properties. In our previous research we proved that a neural gas network is able to cluster both geometric and elastic properties of the objects embedded in a modeled point cloud [11]. In spite of some guidelines that we developed to choose an appropriate map size based on the size of the initial scan and the desired accuracy of the model, the efficiency of such a solution can vary slightly with the characteristics of the objects considered, such as the size of the object, and the number and the size of features. Growing networks eliminate some of these limitations. Such networks add supplementary nodes into the network structure at the position where the accumulated error is the highest and when the number of learning iterations performed is an integer multiple of some predefined value, eliminating the constraint imposed by the fixed map size. As a node is added, another set of iterations is performed before another new node is introduced. Therefore the network grows always at the same rate regardless of the way the input distribution is changing. The growth of the network is terminated when a predefined stopping criterion is met (e.g. a minimum error or a network size limit is reached).

There are several growing self-organizing algorithms proposed in the literature. The most popular are: the growing grid, the growing cell structures, the growing neural gas [12] and the growing hierarchical self-organizing map (SOM) [13], just to mention a few. Several of the advantages of such architectures are that they only use constant parameters and that the training is faster when compared to other neural networks and other clustering algorithms. However, many of these growing architectures are still constrained by predefined network map shape, such as a rectangular grid in the case of the growing grid and the growing hierarchical SOM or k-dimensional hyper-tetrahedrons in the case of growing cell structures. Unlike these, a growing neural gas is a network without fixed dimensionality and has no predefined map. In this case the dimensionality of the network depends on the local dimensionality of the data and may vary within the input space. For this reason, growing neural gas seems a good choice for the application considered here.

The growing neural gas builds a topology, generated using competitive Hebbian learning [14], which inserts an edge between the two closest nodes. The closeness is measured in Euclidian distance from an input signal. There are no restrictions on the topology. Arbitrary edges are allowed and the topology can have different dimensionalities in different parts of the input space. The resulting graph is an induced Delaunay triangulation. This induced Delaunay triangulation has been shown to optimally preserve topology in a very general sense [14].

The growing neural gas algorithm can be described as follows: a new node is added every λ iterations, to support the node with the highest local accumulated error. For each input vector presented to the network, two best matching nodes are selected, whose weights are the closest to the input, based on Euclidean distance. This choice is justified by the fact that placing a new node in the median position between these two matching nodes will decrease the influence of each of the initial large error nodes and therefore will contribute to a

minimization of their future errors. A neighborhood connection is created between them if the connection does not already exist and its age is set to 0. The position of these nodes and the ones of the topological neighbors of the winner unit are moved such that they better fit the input. All edges that are not used increase in age and if the age exceeds a threshold, a_{max}, the corresponding edges are deleted. Any node that has no edge connection is removed as well. After λ iterations, a new node is added to support the node that has accumulated the highest error in the previous steps. The new node is placed between the node with the highest error and one of its neighbors that has the next highest error. The errors of all nodes are globally decreased and the algorithm continues until some stopping criterion is met. A formal description of the algorithm and additional explanations can be found in [12].

The same procedure is employed here as the one proposed for the neural gas solution in [11]. Similar to the neural gas, the growing neural gas is employed to detect areas rich in geometrical features starting from an initial fast scan of different objects under study. Starting from the points collected during a fast scan of an object via an active range finder and an initial configuration of unconnected nodes, the latter move freely over the data space while learning and the model contracts asymptotically towards the points in the input space, respecting their density and thus taking the shape of the objects encoded in the point cloud. This ensures that density of the probing points will be higher in the regions with more pronounced variations in the geometric shape.

B. Regions of Interest Detection

The higher density regions in the growing neural gas are detected by traversing the nodes successively and checking the length of vertices between neighbor nodes. An average value for all these lengths is computed and a threshold is set to this value. All the nodes that are located further away from each other than the value of the threshold are removed from the model. The remaining points identify those regions that require additional sampling. Supplementary data is collected for all these regions and the resulting selectively sampled multi-resolution model is constructed by augmenting the initial sparse low resolution scan with the higher resolution data samples. The procedure can be repeated in several steps to improve the final model.

IV. EXPERIMENTAL RESULTS

The proposed method is tested on 3D range data point clouds of objects. While the point clouds of the objects presented here are collected for a fixed scanner position with only a single viewpoint, the procedure can be employed unchanged for multi-viewpoint data or from data coming from different scanning systems as long as it comes in (*x,y,z*) format. Apart from the real data, sets of synthetic data obtained from the interpolation on a higher resolution mesh of a sparse scan are used to train the network. The objects used for testing are shown in Fig. 1.

Starting from an initial fast, sparse scan of each object under study, a growing neural gas network is employed to model the data in the point cloud, in the form of (*x, y, z*) coordinates. The data set is normalized prior to the mapping such that its variance is unity. Testing is performed for several resolutions of the initial fast/sparse scan in order to identify how the resolution of this scan influences the modeling results and what would be the smallest scan to start with that allows for the modeling of fine features in the modeled objects.

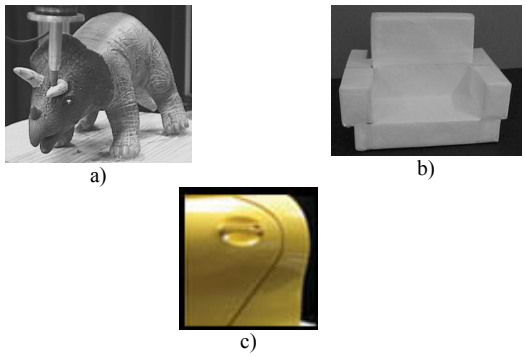

Fig. 1. a) Toy triceratops, b) foam chair, and c) mock-up car door used for testing.

Fig. 2 shows the enlarged best modeling results for a low resolution initial scan of 3065 points, shown in Fig. 2a, and for a medium low resolution initial scan of 6113 points, presented in Fig. 2b, for $\lambda=3$ and $a_{max}=20$.

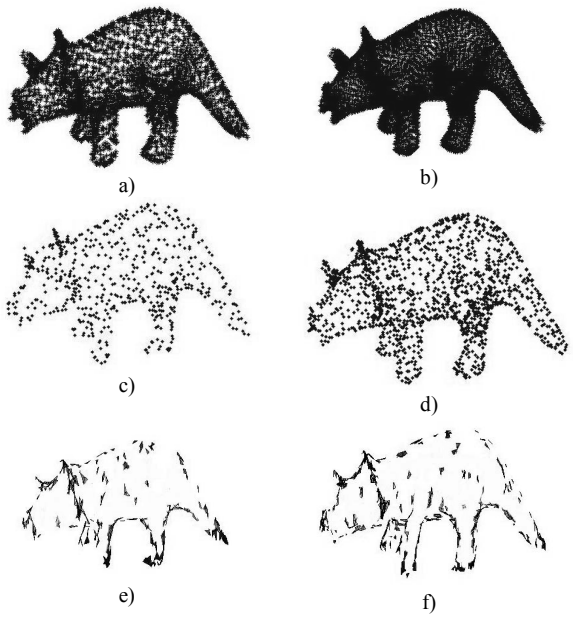

Fig. 2. Initial scan at (a) low resolution and (b) medium low resolution, growing neural gas model of (c) 757 points and (d) 1410 points, and detected regions of interest for further sampling for (e) low resolution and (f) medium low resolution models.

The growing neural gas network, having as inputs these initial sparse point clouds, builds a topology that respects the density of points in the initial point cloud. The topology can be seen as compressed mappings for the initial dataset, as depicted in Fig. 2c and 2d for the low and medium low resolution initial scans respectively. The areas with dense geometrical features found in these mappings are shown in Fig. 2e and 2f respectively. The dense feature areas are much better identified and contoured for the higher resolution model, in Fig. 2f. However, in both cases, the network is able to identify, apart from the contours of the model, the areas around the head and horns of the triceratops as areas worth further scanning, as it is expected.

The chair represents an object without many features and its initial dataset contains raster-like distributed sampling points. Fig. 3 presents the modeling results using a growing neural gas for a low (3065 points) and a medium (6113 points) resolution initial scans on the chair, obtained for $\lambda=3$ and $a_{max}=20$.

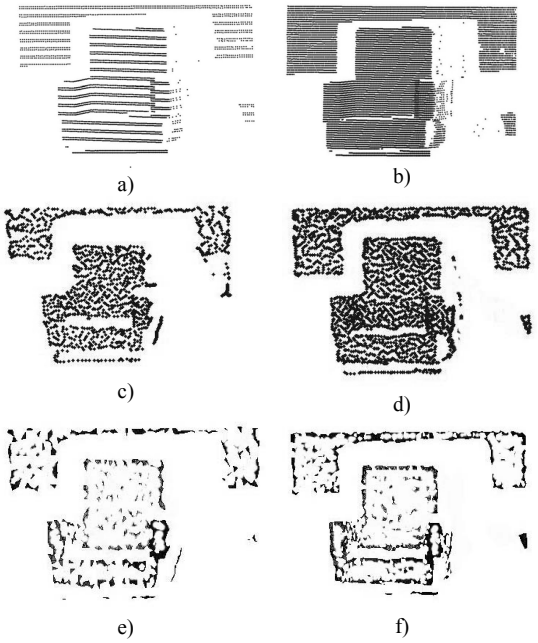

Fig. 3. Initial scan at (a) low resolution and (b) medium resolution, growing neural gas model of (c) 1243 points and (d) 2826 points, and detected regions of interest for further sampling for (e) low resolution and (f) medium resolution models.

The same parameters are used as in the case of the triceratops and the results are evaluated for different sizes of the initial scan. For both cases, it shows the detected regions of interest in the growing neural gas map (Fig. 3e for the low resolution and Fig. 3f for the medium resolution). As it can be seen, the network is able to detect the features in both cases in spite of some noise in the modeling results.

As a last example, a fast scan of medium resolution on the door is initially performed to obtain the 16384 points medium resolution scan as shown in Fig. 4a. The resulting growing neural gas mapping is depicted in Fig. 4b, the areas of high density in this mapping in Fig. 4c, and the detected regions of interest are highlighted in Fig. 4d, neglecting the contour areas.

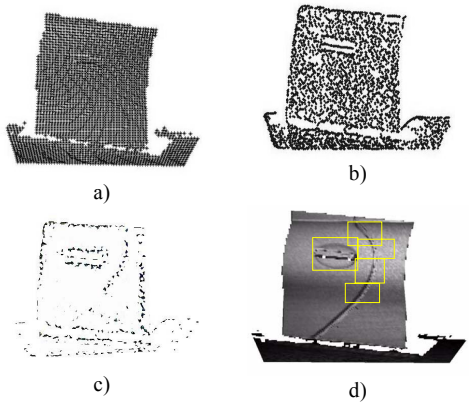

Fig.4. The mock-up door (a) point cloud, (b) growing neural gas mapping, (c) high density areas, and (d) the detected regions of interest.

As in the case of neural gas, the same procedure can be repeated for each of the regions of interest detected in the previous step. Each region is provided as input to a growing neural gas network in order to further detect fine details that are worth to be scanned at a higher resolution. Fig. 5 presents the details of the high resolution rendered model of the door for the selected regions in the previous step.

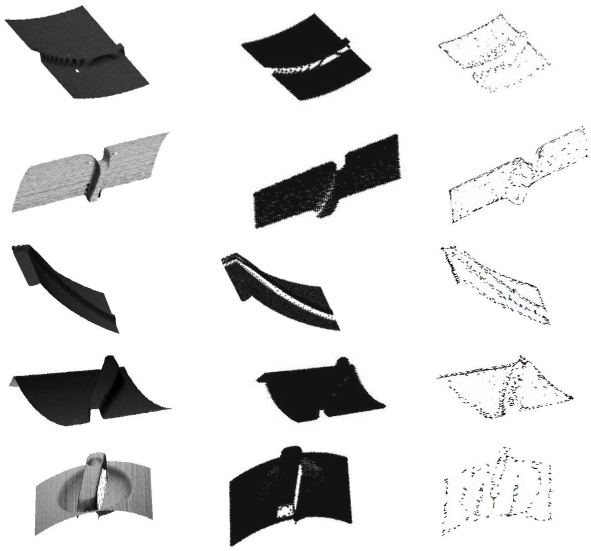

Fig. 5. Different views of rendered selected regions (first column), point clouds of selected regions (second column) and detected regions of interest for each view (third column).

For each of the selected regions it shows the growing neural gas model for $\lambda=3$ and $a_{max}=20$ and the regions of interest detected at the second stage for further scanning, identified as high density areas in the growing neural gas model. The average error is of order e^{-6} for each of the regions.

All the presented examples show the capability of the growing neural gas map to capture the fine details in the sparsely collected point clouds of all the objects under study. By finding the higher density areas in the growing neural gas map, the proposed selective sampling procedure is able to identify and guide the sensor to collect only measurements in those regions that are of interest for the improvement of accuracy of the final multi-resolution models.

V. COMPARISON WITH THE NEURAL GAS SOLUTION

Although the neural gas and growing neural gas algorithms both present self-organizing attributes, are similar in approach and are based on the same ideas, there are differences in terms of required user intervention, accuracy of results, training time and obtained errors. These differences are summarized below.

To begin with, the growing neural gas eliminates the need for the map size to be decided prior to learning as in the case of neural gas. Moreover, by comparing the final map size obtained with growing neural gas and the one obtained with neural gas, it can be seen in Table 1 that generally the size of the growing neural gas map (the number of nodes in the resulting graph) is smaller than the one required by neural gas in order to obtain similar modeling results.

Table 1. Approximate network map sizes for different sizes of initial scans with neural gas (NG) and growing neural gas (GNG).

Size of initial point cloud (number of points, N)	*Approximate map size with NG*	*Approximate map size with GNG*
2000-3000	60%-100%N	20-45%N
3000-4000	50%-90%N	20-45%N
4000-5000	30%-70%N	20-45%N
5000-6000	20%-60%N	16-49%N
6000-7000	15%-50%N	16-49%N
over 16000	10%-40%N	10-40%N

The average network map sizes for different initial scans, computed as the average value of the network map sizes for the range of values that provide reasonably good modeling results and for all the objects under study, as per Table 1, are shown in Fig. 6.

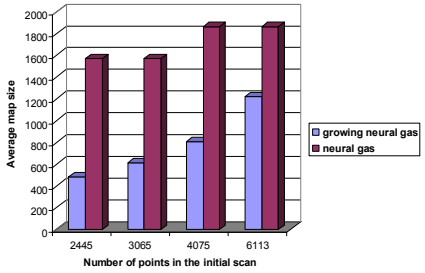

Fig.6. Comparison between growing neural gas and neural gas based on map size.

In spite of the lower network map size, the accuracy of growing neural gas models is higher when compared to neural gas, as depicted in Fig. 7. The relative error is computed as an average distance between each data vector and its winning neuron and therefore shows how close the modeled data is to the initial scan point cloud. The average error is computed as the average relative error for all objects under study, as in the case of the network map size.

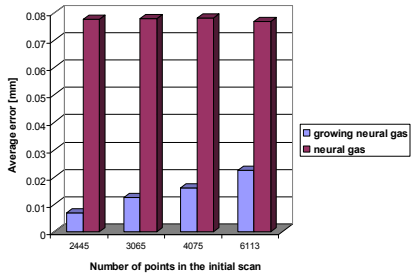

Fig. 7. Comparison between growing neural gas and neural gas based on errors.

In terms of training time, the time required to build the model is also generally lower for growing neural gas, as shown in Fig. 8.

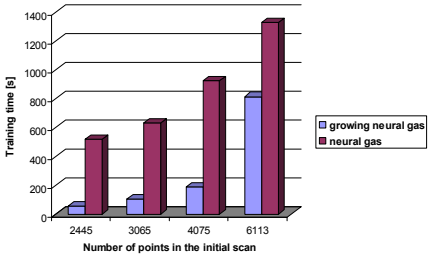

Fig. 8. Comparison between growing neural gas and neural gas based on training time.

However, since the map obtained by growing neural gas is evenly distributed over raster-like object point clouds, the relevant areas for additional scanning are slightly harder to identify and they result in higher noise in the characterization of relevant features, as it can be seen in Fig. 9. The first column of Fig. 9 shows the best modeling cases for the neural gas while the second column presents growing neural gas models. When comparing the results in Fig. 9, it can be noticed that the edges are clearer on the contours in Fig. 9a-c, representing the high density areas detected in the neural gas map than those in Fig. 9d-f that represent the high density areas in the growing neural gas map. As such, the results in the second column are slightly noisier. This phenomenon is alleviated in the case of neural gas model by slightly over-sizing the map dimensions and stopping the adaptation early enough not to allow the output space to become evenly distributed. Such a mechanism is impossible to be established in the case of growing neural gas as the points in the output space are added iteratively to support the node that has accumulated the highest error in the previous steps. The new

node is placed between the node with the highest error and the one of its neighbors with the next highest error. Therefore the error between the input space and the map being built is always decreased. This implies that the model will respect the density of points in the point cloud and cover evenly the input space, but gives less control on the training duration.

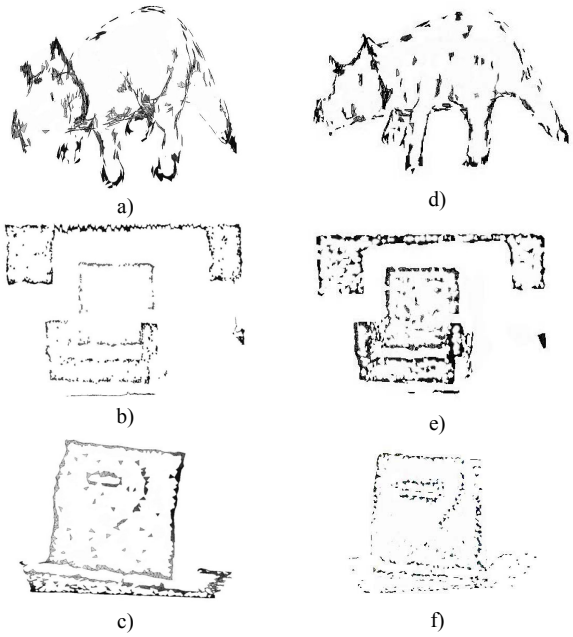

Fig. 9. Higher feature density areas identified in the neural gas map (first column) for (a) triceratops (b) chair and (c) door, and in the growing neural gas map (second column) for (d) triceratops, (e) chair and (f) door.

From this experimentation, the growing neural gas reveals to be faster, to lead to lower errors in mapping and to require less user interaction in the modeling procedure. But it gives slightly noisier results for geometrical feature detection as required for further sampling regions selection. Therefore the growing neural gas is an appropriate choice when more compact object models are desired, and when the user is not willing to interfere at all in the modeling procedure. On the other hand, neural gas provides clearer definition of the regions for further scanning, especially on edges but requires some trial-and-error settings in order to provide the best results. Therefore this choice is appropriate when the user is interested in accurately finding features over the objects.

VI. CONCLUSIONS

The growing neural gas eliminates the need of the map size to be decided prior to learning, as in the case of neural gas. During adaptation the network adds iteratively nodes to the structure to better fit the data provided as input and is able, in all the cases under study to identify the regions of further interest for scanning. All the examples show the ability of the growing neural gas map to capture the fine details in the sparsely collected point clouds of the objects under study. By finding the high density areas in the growing neural gas map, the proposed selective sampling procedure is able to automatically identify and guide the vision sensors to collect only measurements in those regions that are of interest for the improvement of accuracy of the obtained models, saving at the same time large amount of less relevant data in the scans. The growing neural gas solution is faster, reaches lower errors and does not require user intervention for the selection of an appropriate map size when compared to the previously proposed neural gas solution.

Further research is directed towards the use of the growing neural gas network for deformable objects sampling.

ACKNOWLEDGEMENTS

The authors wish to acknowledge the support from Communications and Information Technology Ontario Centre of Excellence, and from the Natural Sciences and Engineering Research Council of Canada. The authors also want to thank Dr. Chad English from Neptec Design Group Inc. and Dr. Jochen Lang for providing access to high resolution range data and the triceratops model.

REFERENCES

[1] D. Nehab, and P. Shilane, "Stratified Point Sampling of 3D Models", *Eurographics Symposium on Point-Based Graphics*, M. Alexa, S. Rusinkiewicz (Eds.), pp. 49-56, 2004.

[2] R. Dillmann, S. Vogt, and A. Zilker, "Data Reduction for Optical 3D Inspection in Automotive Applications", *Proc. IEEE Int. Conf. Multi-Sensor Fusion & Integration for Intelligent Systems,* pp.159-164, 1999.

[3] K. Lee, H. Woo, and T. Suk, "Point Data Reduction Using 3D Grids", *Int. Journal of Adv. Manuf. Tech.,* vol.18, pp.201-210, Springer, 2001.

[4] A. Kalaiah, and A. Varshney, "Statistical Point Geometry", *Proc. of Eurographics Symp. Geometry Processing*, K. Kobbelt, P. Schroder and H. Hoppe (Eds.), pp. 107 - 115, 2003.

[5] M. Pauly, M. Gross, and L.P. Kobbelt, "Efficient Simplification of Point-Sampled Surfaces", *Proc. IEEE Conf. Visual.*, pp. 163-170, 2002.

[6] D. Uesu, L. Bavoil, S. Fleishman, J. Shepherd and C. T. Silva, "Simplification of Unstructured Tetrahedral Meshes by Point Sampling", *Proc. IEEE Int. Workshop Volume Graphics*, E. Gröller, I. Fujishiro (Eds.), pp. 157- 238, 2005.

[7] H. Song and H.-Y. Feng, "A Point Cloud Simplification Algorithm for Mechanical Part Inspection", *Information Technology for Balanced Manufacturing Systems*, W. Shen (Ed.), Springer, pp. 461-468, 2006.

[8] D. K. Pai, K. van den Doel, D. L. James, J. Lang, J. E. Lloyd, J. L. Richmond, and S. H. Yau, "Scanning Physical Interaction Behavior of 3D Objects", *Proc. Computer Graphics and Interactive Techniques,* pp. 87-96, 2001.

[9] J. Lang, D.K. Pai, and R. J. Woodham, "Acquisition of Elastic Models for Interactive Simulation", *Int. Journal of Robotics Research*, vol. 21, no.8, pp.713-733, 2002.

[10] D. MacKinnon, V. Aitken, and F. Blais, "Adaptive Laser Range Scanning using Quality Metrics", *Proc. IEEE Int. Instr. and Meas. Technology Conf.,* pp.348-353, Victoria, BC, May 2008.

[11] A.-M. Cretu, P. Payeur and E.M. Petriu, "Selective Vision Sampling with Neural Gas Networks", *Proc. IEEE Int. Instr. and Meas. Technology Conf.*, pp. 478-483, Victoria, Canada, May 2008.

[12] B. Fritzke, "Unsupervised Ontogenic Networks", in *Handbook of Neural Computation*, Eds. E. Fiesler, R. Beale, IOP Publishing Ltd and Oxford University Press, C2.4, 1997.

[13] M. Dittenbach, D. Merkl and A. Rauber, "The Growing Hierarchical Self-Organizing Map", *Proc. Int. Joint Conf. Neural Networks*, pp. VI-15 - VI-19, Como, Italy, 2000.

[14] T.M. Martinetz, "Competitive Hebbian Learning Rule Forms Perfectly Topology Preserving Maps", *Proc. Int. Conf. Artificial Neural Networks,* Springer, Amsterdam, pp. 427-434, 1993.